Residual Performance of Structural Steel After Cyclic Plastic Deformation and Strain Aging

Haruka Nakagawa[1(✉)], Kayo Taniguchi[1], Shaoqi Yang[2], Tetsuhiro Asari[1], and Taichiro Okazaki[1]

[1] Hokkaido University, Sapporo, Hokkaido 064-0801, Japan
pippi-haru@eis.hokudai.ac.jp
[2] Formerly Hokkaido University, Sapporo, Hokkaido 064-0801, Japan

Abstract. The sustainability of steel construction can be improved dramatically by establishing reuse, in a new structure, steel components procured from an older structure. To achieve this goal, the residual performance of used steel must be evaluated. For seismic areas, the residual performance after experiencing an earthquake, large or small, must be quantified. Therefore, the residual performance of hot rolled I-shapes, of grades SS400, SN400B and SN490B, after plastic deformation and strain aging was examined through three test series: (I) tension coupon tests; (II) cyclic tension-and-compression coupon tests; and (III) cyclically loaded beam tests. The tests were conducted in two phases: pre loading to predetermined plastic deformation, and subsequently, after curing for 1 or 3 months at ambient temperature, loading to larger plastic deformation. The SS400 with free nitrogen content of 0.006 wt% saw substantial strain aging effects, while SN400B and SN490B with free nitrogen content of 0.003 and 0.002 wt% saw smaller effects. In the beam tests, pre-loading to ±0.02 rad resulted in up to 25% increase in yield strength but little change in maximum strength and plastic deformation capacity. Residual deformation of the beam was within geometric tolerances after cyclic loading to ±0.01 rad, but exceeded some tolerance items after cyclic loading to ±0.02 rad.

Keywords: Reuse · Residual performance · Plastic deformation · Strain aging · Cyclic-loading tests · Beams

1 Introduction

Steel is very well suited for sustainable construction owing to its recyclable and durable properties. Today, in Japan, nearly all structural steel is recycled after the service life of the building is ended. However, the recycle process from steel scrap to new steel, using the electric-arc furnace, consumes abundant energy and emits abundant carbon dioxide. The sustainability of steel construction can be further promoted by establishing reuse: procuring steel components from a building during demolition, refurbishing and then reusing those components in a new structure. In order to establish steel reuse, amid modern quality control requirements, the residual performance of used steel must be evaluated. Unless exposed to corrosive environments, which is limited to special use, structural steel in buildings does not degrade with time. In most cases, reusability may be judged based on visual inspection and geometric check against tolerance limits.

F. M. Mazzolani et al. (Eds.): STESSA 2022, LNCE 262, pp. 157–165, 2022.
https://doi.org/10.1007/978-3-031-03811-2_12

Segments severely altered by welding, trimming, protrusions, etc., may be unsuitable for reuse. However, in a seismically active environment like Japan, scientific basis is needed to judge the reusability of steel affected by earthquakes, large or small: severe earthquakes can cause plastic deformation in steel components, which, combined with ensuing strain aging, degrade the ductile properties of those steel components. Therefore, towards the larger goal of promoting steel reuse, an experimental program is conducted to quantify the effect of plastic deformation and strain aging on the residual seismic performance of structural steel.

Strain aging in low carbon steel is caused by segregation of interstitial carbon and nitrogen atoms to form atmospheres around dislocations [1]. The extent of strain aging is controlled by the chemical composition of the steel [2, 3] and curing environment [4]. Kaufmann et al. [5] report from tension coupon tests on steels produced in different eras and different milling processes that, in the range of 2 to 12%, larger pre-strain caused 20 to 40% larger increase in yield strength. Mojtaba [6] report for Japanese SN490B steel that increase in yield strength was independent of the amount of pre-strain and that strain hardening rate did not change with strain aging. Yamada et al. [7] observed for SS400 steel that strain aging may saturate at 3 months under ambient temperature. They also observed from cyclic-loading tests of beam-to-column connections made of SS400 steel that strain aging can result in a favorable distribution of tension properties to promote yielding in regions away from critical welds.

2 Test Plan

Hot rolled, H-500×200×10×16 sections of three different structural steel grades, Japanese Industry Standard (JIS) SS400, SN400B and SN490B, all produced by the blast furnace process, were selected for the study. These are among the most common steel grades in Japan: SS400 (specified yield strength, $\sigma_y \geq 235$ N/mm^2) is an old grade introduced in 1952; SN400B ($235 \leq \sigma_y \leq 355$ N/mm^2) and SN490B ($325 \leq \sigma_y \leq 455$ N/mm^2) are widely used for primary load-resisting systems. Table 1 lists the mechanical properties and key chemical composition of the steel samples. The mechanical properties were established from the tension coupon tests described later. Carbon content was taken from mill test reports. The total and free nitrogen content was measured according to *JIS G 1228: Iron and steel – Methods for determination of nitrogen content*. For all three samples, free nitrogen content was close to total nitrogen content. Between the three grades, SS400 had notably larger total and free nitrogen content than SN400B or SN490B.

Table 2 summarizes the tests completed so far. The same steel samples were used for three different test series: (I) monotonic tension coupon tests, (II) cyclic tension-and-compression coupon tests and (III) cyclically loaded beam tests. At the time of this writing, (I) is completed, and (II) and (III) are underway.

For Series (I), which is completed, JIS 1A tension coupons were extracted from the flange and web of the I-sections. An extensometer was devised to measure engineering strain over the standard gauge length of 200 mm. The coupons were pre strained to three different values, 2, 4 and 8%, and then cured at room temperature for 1 or 3 months. After curing, the pre-strained coupons were tensioned to fracture.

Figure 1a shows the test setup for Series (II), which is underway. JIS 1A tension coupons extracted from the flanges are loaded in cyclic strain amplitudes increasing as ±0.5, ±1.0, ±1.5, ±2.0, ±2.5, ±3.0, ±3.5 to ±4.0%, each amplitude repeated twice. A buckling-restraining system is used to control buckling under compression. In the

Table 1. Mechanical and chemical properties.

Mechanical property or chemical composition	Steel Grade					
	SS400		SN400B		SN490B	
	Flange	Web	Flange	Web	Flange	Web
Yield strength [N/mm^2]	300	332	284	322	344	358
Tensile strength [N/mm^2]	448	462	457	472	521	522
Elongation [%]	31	28	33	29	29	25
Yield-to-tensile ratio	0.67	0.72	0.62	0.68	0.66	0.69
Carbon content [wt%]	0.15		0.16		0.16	
Total nitrogen content [wt%]	0.0073		0.0031		0.0028	
Free nitrogen content [wt%]	0.006		0.003		0.002	

Table 2. Completed tests.

Series	Steel Grade		
	SS400	SN400B	SN490B
(I)	0%, 2%, 4%, 8%	0%, 2%, 4%, 8%	0%, 2%, 4%, 8%
(II)	±0%, resumed-±1%, resumed-±2%, restarted-±1%, restarted-±2%	±0%, restarted-±2%	±0%, restarted-±2%
(III)	±0 rad, resumed-0.01 rad, resumed-±0.02 rad, restarted-±0.02 rad	±0 rad, restarted-±0.02 rad	±0 rad, restarted-±0.02 rad

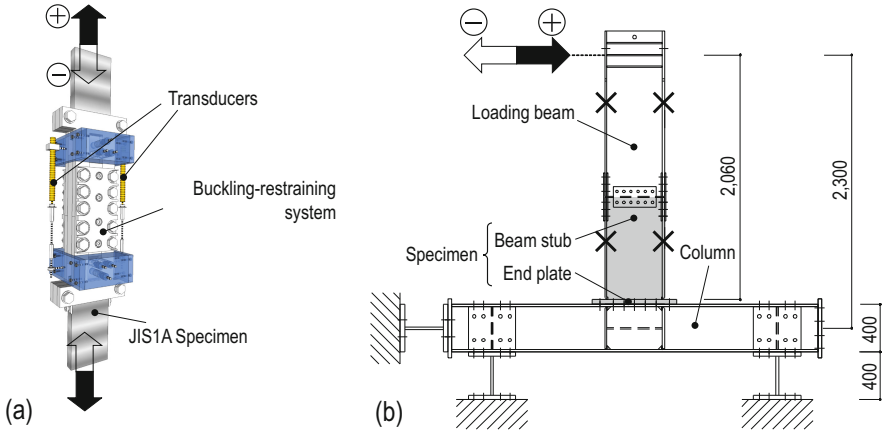

Fig. 1. Test setup: (a) cyclic-loading coupon tests; (b) cyclic-loading beam tests.

first stage, the coupon is loaded to a strain amplitude of ±1.0 or ±2.0%, unloaded to zero strain, then cured at room temperature for 3 months. In the second stage, the cyclic protocol is resumed from where the first stage ended or restarted from the beginning.

Figure 1b shows the test setup for Series (III), which is underway. The specimen comprises a beam stub welded to an end plate using the no-weld-access-hole beam-to-column moment connection detail. The beam and loading beam are laterally braced at the locations indicated by "X" marks. Loading is controlled according to the US cyclic loading program for prequalification tests of moment-frame connections: cyclic story-drift angle is increased from ±0.00375, ±0.005, ±0.0075, ±0.01, ±0.015, ±0.02, ±0.03, to ±0.04 rad. Three cycles are repeated for each angle up to ±0.01 rad, and afterwards two cycles are repeated for each angle. In the first stage, the specimen is loaded to a cyclic angle of ±0.01 or ±0.02 rad, unloaded to zero story drift, and then cured at room temperature for 3 months. In the second stage, the cyclic protocol is resumed from where the first stage ended or restarted from the beginning.

All series include a specimen loaded with no pre-strain to provide data on performance without strain aging. For each steel grade, all specimens were extracted from the same heat of steel.

3 Monotonic Coupon Tests

Figure 2 shows stress versus strain relationships obtained from Series (I) for flanges. The coupons were pre-strained to 0 (no pre strain), 2, 4 or 8%, cured for 1 or 3 months, then tensioned to fracture. The mechanical properties listed in Table 1 were established from the coupon indicated in the figures as 0% pre strain. Change in tension properties due to strain aging was observed as reappearance of yield plateau, rise in yield strength, rise in tensile strength, and reduction in elongation with respect to the original properties. For all three grades, larger pre strain resulted in larger change in tension properties: 8% pre strain resulted in 30 to 50% increase in yield strength due to strain hardening, and an additional 3 to 18% increase due to strain aging. The change in tension properties was more pronounced for SS400 than for SN400B or SN490B: 8% pre-strain resulted in 5 to 7% increase in tensile strength and 10 to 19% reduction in elongation for SS400 but no change in tensile strength and elongation for SN400B or

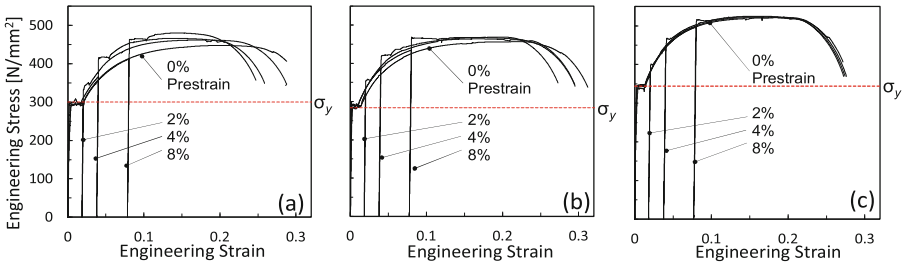

Fig. 2. Stress vs. strain relationships from tension coupon tests, extracted from flange, with 3-month curing: (a) SS400 steel; (b) SN400B steel; and (c) SN490B steel.

SN490B. The results correlated with the free nitrogen content listed in Table 1: the free nitrogen content was 0.006 wt% for SS400 but 0.003 and 0.002 wt%, respectively, for SN400B or SN490B. Although not shown here, no significant difference was observed between curing periods of 1 or 3 months. The change in yield strength and elongation for SS400 steel was consistent with the report by Yamada et al. [7]. The rise in tensile strength was notably smaller than the results reported by Yamada et al. [7] and Pense [4].

4 Cyclic Coupon Tests

Figure 3 shows stress versus strain relationships obtained from Series (II). Four different loading cases are shown for SS400: (1) no pre-strain; (2) restarting the cycles after pre strain to ±2%; (3) resuming the cycles after pre strain to ±1%; and (4) resuming the

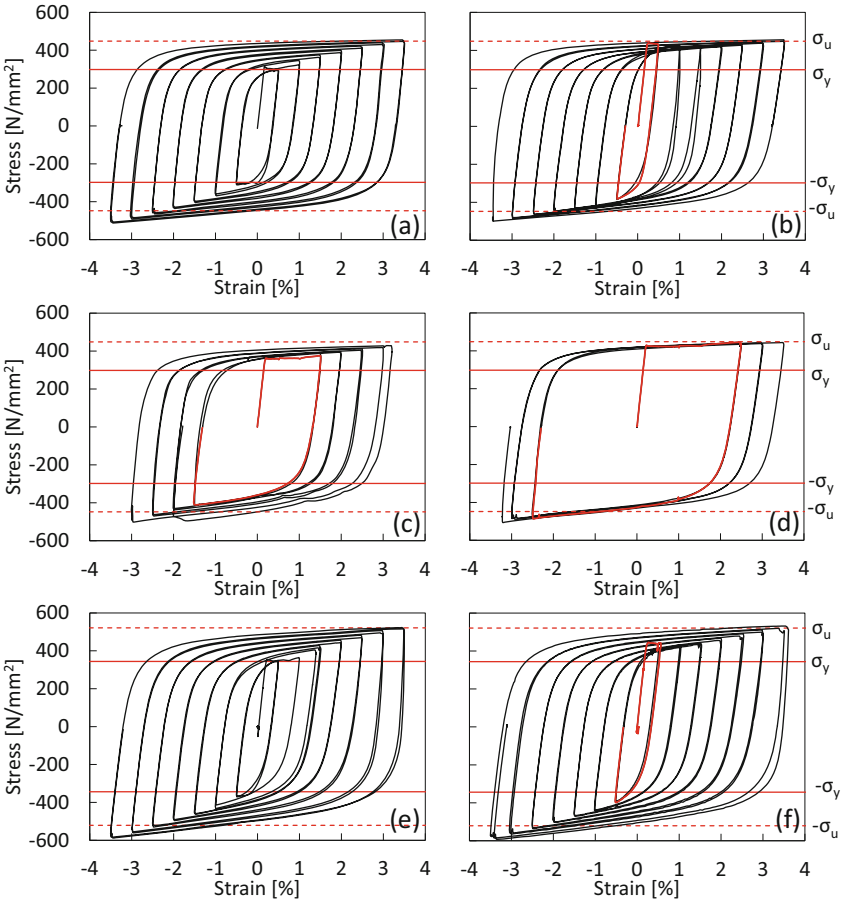

Fig. 3. Stress-strain relationships from cyclic coupon tests: (a) SS400 with no pre-strain; (b) SS400 restarted after ±2%; (c) SS400 resumed after ±1%; (d) SS400 resumed after ±2%; (e) SN490B with no pre-strain; and (f) SN490B resumed after ±2%.

cycles after pre strain to ±2%. Two cases among the four, (1) and (2), are shown for SN490B. The plots omit the pre-strain cycles and show only the second-stage response. Most tests were terminated before the ±4% cycles when deformation of the coupon started to disrupt measurement. The larger stress in compression than tension is believed to be due to contact between the coupon and buckling-restraining system.

Clear and consistent trends are seen in these examples: strain aging tends to exhaust the room for stress increase with loading cycle, i.e., isotropic hardening. As in Series (I), reappearance of yield plateau and rise in yield strength was noted in the first half cycle, in tension, after curing. Larger pre strain resulted in larger rise in yield strength and larger loss of isotropic hardening. The loss of isotropic hardening was more prominent for SS400 than for SN490B. The largest measured tensile stress was no greater than the tensile strength established from regular tension coupon tests.

5 Cyclic-Loading Beam Tests

Figure 4 shows the cyclic-loading response obtained from Series (III). The relationship between beam-end moment and story drift angle is plotted for four SS400 specimens and two SN490B specimens. Only the second-stage response is shown. The plastic moment, M_p, based on the yield strength listed in Table 1, is shown for reference. When no pre strain was introduced, yielding started from the ±0.0075-rad cycles, maximum resistance was recorded between ±0.02 and ±0.03-rad, and, at the end of the ±0.04 rad cycles, the resistance had dropped by 25 to 33% from the maximum recorded value but maintained M_p. The primary cause of strength degradation was local flange and web distortion.

The resumed or restarted SS400 specimens responded elastically to a resistance higher than M_p. The resumed specimens exhibited an apparent yield plateau during the first half cycle after curing, which was not seen in the specimen with no pre strain. Pre strain to ±0.02 rad resulted in plateau strength exceeding M_p by 20% due to strain hardening and an additional 22% due to strain aging. The difference caused by pre strain diminished after a small number of loading cycles. Little difference in maximum resistance was recorded. All four SS400 specimens exhibited very similar behavior during the ±0.04-rad cycles. In contrast to SS400, the residual performance of SN490B specimen after pre-strain to ±0.02-rad was nearly identical to the original, in size of initial elastic domain, story drift angle when maximum resistance was recorded, or rate of strength degradation. For both SS400 and SN490B, pre strain to ±0.02 rad had little effect on the plastic deformation capacity of the beam.

At the end of pre-strain cycles to ±0.01 or ±0.02 rad, the specimens were brought to zero chord rotation and cured for 3 months. During curing, the specimens were examined by visual inspection and 3D digital reconstruction. Apart from flaking of mill scale, no evidence of plastic loading history was recognized by visual inspection. Table 3 summarizes the measured dimensions checked against limits by *ASTM A6*

Standard specification for general requirements for rolled structural steel bars, plates, shapes, and sheet piling and *JIS G 3192 Dimensions, mass and permissible variations of hot rolled steel sections*. For the one sample listed, the beam remained within geometric limits after pre strain to ±0.01 rad. However, the beams violated limits such as camber, sweep and web out-of-flatness after pre-strain to ±0.02 rad.

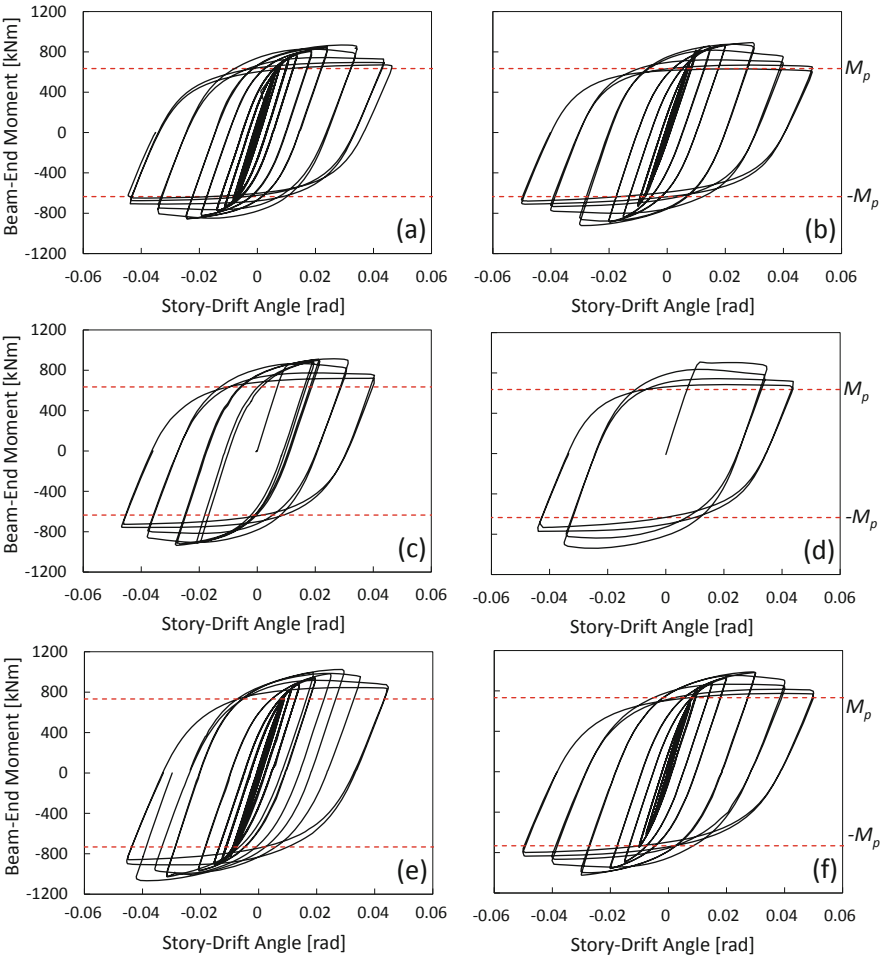

Fig. 4. Loading curves obtained from cyclically-loaded beam tests: (a) SS400 with no pre-strain; (b) SS400 restarted after ±0.02 rad; (c) SS400 resumed after ±0.01 rad; (d) SS400 resumed after ±0.02 rad; (e) SN490B with no pre-strain; (f) SN490B restarted after ±0.02 rad.

Table 3. Geometric limits vs. out of straightness measured after first-stage loading.

Item	Limits		Measured maximum value				
	JIS	ASTM	SS400 0.01 rad	SS400 0.02 rad	SS400 0.02 rad	SN400B 0.02 rad	SN490B 0.02 rad
Camber [mm]	2.1	2.2	2.0	**2.8**	**2.2**	**4.0**	1.6
Sweep [mm]	2.1	2.2	2.0	**3.6**	2.0	1.5	**3.0**
Depth over theoretical [mm]	N.A.	6.4	2.7	2.5	2.6	N.A.	3.5
Web out-of-flat [mm]	2.5	N.A.	1.6	**3.6**	1.6	1.4	1.2
Flange out-of-flat [mm]	1.5	N.A.	1.2	1.3	1.3	1.3	0.6
Flange 1 out-of-square [mm]	2.4	N.A.	1.9	**2.6**	2.1	1.2	1.4
Flange 2 out-of-square [mm]	2.4	N.A.	1.5	2.0	1.7	1.1	1.3
Flanges out-of-square [mm]	N.A.	7.9	3.4	4.6	3.8	2.2	2.8

6 Summary

An experimental program is underway to examine the effect of plastic deformation and strain aging on the residual seismic performance of structural steel components. The program includes three test series on steel extracted from SS400, SN400B and SN490B steel: (I) tension coupon tests; (II) cyclic tension-and-compression coupon tests; and (III) cyclically loaded beam tests. Each test included pre-strain loading, curing for 1 or 3 months at ambient temperature, and second-stage loading. Key findings are listed below.

- Among the three steel samples, SS400 with free nitrogen content of 0.006 wt% showed the most profound difference between residual and original performance, while SN400B and SN490B with free nitrogen content of 0.003 and 0.002 wt%, respectively, showed less change.
- Strain aging did not seem to alter kinematic hardening but seemed to reduce isotropic hardening under cyclic loading.
- The cyclically loaded beam tests suggest that strain hardening and strain aging produced by pre-strain loading up to ± 0.01 or ± 0.02-rad does not affect the cyclic loading response at ± 0.04 rad, and therefore, does not affect the plastic deformation capacity of the beam.
- After pre-strain loading up to ± 0.02-rad and unloading to zero chord rotation, residual deformation of beams was not visually recognizable but violated some of the geometric requirements for newly produce steel.

References

1. Cottrell AH, Bilby BA (1949) Dislocation theory of yielding and strain ageing of iron. Proc Phys Soc Sect A 62(1–349 A):49–61
2. Wilson DV, Russell B (1960) The contribution of atmosphere locking to the strain-aging of low carbon steels. Acta Metall 8(1):36–45

3. Ono T, Murayama K, Masuda K, Sato A, Yokokawa T (2000) The experimental study on the effect of trace elements on toughness of steel plate for building structure. J Struct Constr Eng 536:157–162 (in Japanese)
4. Pense A (2004) HPS corrugated web girder fabrication innovations, Final report, Part 4: Literature and experimental study of strain aging in HPS and other bridge steels. Center for Advanced Technology for Large Structural Systems, Bethlehem, USA, 7
5. Kaufmann EJ, Metrovich B, Pense AW (2001) Characterization of cyclic inelastic behavior on properties of A572 Gr. 50 and A36 rolled sections. ATLSS Report No. 01–13, Bethlehem, USA
6. Mojtaba MA (2015) Static strain aging in low carbon ferrite-pearlite steel: forward and reverse loading. Electronic Theses and Dissertations (ETDs), University of British Columbia, Canada
7. Yamada S, Takeuchi A, Kishiki S, Watanabe A (2006) Hysteresis behavior of steel affected by strain aging. Summary of Technical Papers of Year 2006 Annual Meeting, Architectural Institute of Japan, pp 927–930. (in Japanese)